

Homotopic curve shortening and the affine curve-shortening flow*

Sergey Avvakumov[†]

Gabriel Nivasch[‡]

Abstract

We define and study a discrete process that generalizes the convex-layer decomposition of a planar point set. Our process, which we call *homotopic curve shortening* (HCS), starts with a closed curve (which might self-intersect) in the presence of a set $P \subset \mathbb{R}^2$ of point obstacles, and evolves in discrete steps, where each step consists of (1) taking shortcuts around the obstacles, and (2) reducing the curve to its shortest homotopic equivalent.

We find experimentally that, if the initial curve is held fixed and P is chosen to be either a very fine regular grid or a uniformly random point set, then HCS behaves at the limit like the affine curve-shortening flow (ACSF). This connection between ACSF and HCS generalizes the link between ACSF and convex-layer decomposition (Eppstein et al., 2017; Calder and Smart, 2020), which is restricted to convex curves.

We prove that HCS satisfies some properties analogous to those of ACSF: HCS is invariant under affine transformations, preserves convexity, and does not increase the total absolute curvature. Furthermore, the number of self-intersections of a curve, or intersections between two curves (appropriately defined), does not increase. Finally, if the initial curve is simple, then the number of inflection points (appropriately defined) does not increase.

1 Introduction

Let \mathbb{S}^1 be the unit circle. In this paper we call a continuous function $\gamma : [0, 1] \rightarrow \mathbb{R}^2$ a *path*, and a continuous function $\gamma : \mathbb{S}^1 \rightarrow \mathbb{R}^2$ a *closed curve*, or simply a *curve*. If γ is injective then the curve or path is said to be *simple*. We say that two paths or curves γ, δ are ε -*close* to each other if their Fréchet distance is at most ε , i.e. if they can be re-parametrized such that for every t , the Euclidean distance between the points $\gamma(t), \delta(t)$ is at most ε .

1.1 Shortest homotopic curves

Let P be a finite set of points in the plane, which we regard as obstacles. Two curves γ, δ that avoid P are said to be *homotopic* if there exists a way to continuously transform γ into δ while avoiding P at all times. And two paths γ, δ that avoid P (except possibly at the endpoints) and satisfy $\gamma(0) = \delta(0), \gamma(1) = \delta(1)$ are said to be *homotopic* if there exists a way to continuously transform γ into δ , without moving their endpoints, while avoiding P at all times (except possibly at the endpoints). We extend these definitions to the case where γ avoids obstacles but δ does not, by requiring the continuous transformation of γ into δ to avoid obstacles at all times except possibly at the last moment.

*A preliminary version of this article appeared in *Proc. 36th Int. Symp. Computational Geometry (SoCG'20)*, article 12, 15 pages, 2020.

[†]savvakumov@gmail.com. Department of Mathematical Sciences, University of Copenhagen, Copenhagen, Denmark. Has received funding from the Austrian Science Fund (FWF), Project P31312-N35, and the European Research Council under the European Union's Seventh Framework Programme ERC Grant agreement ERC StG 716424 - CAsE.

[‡]gabrieln@ariel.ac.il. Ariel University, Ariel, Israel.

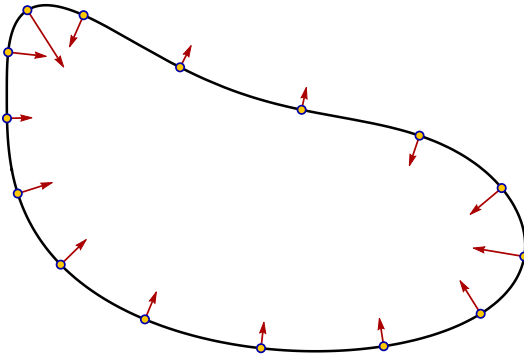


Figure 1: Affine curve-shortening flow. The arrows indicate the instantaneous velocity of different points along the curve at the shown time moment.

For every curve (resp. path) γ in the presence of obstacles there exists a unique shortest curve (resp. path) δ that is homotopic to γ . The problem of computing the shortest path or curve homotopic to a given piecewise-linear path or curve, under the presence of polygonal or point obstacles, has been studied extensively. A simple and efficient algorithm for this task is the so-called “funnel algorithm” [14, 28, 29, 30]. See also [8, 10, 20].

1.2 The affine curve-shortening flow

In the *affine curve-shortening flow*, a smooth curve $\gamma \subset \mathbb{R}^2$ varies with time in the following way. At each moment in time, each point of γ moves perpendicularly to the curve, towards its local center of curvature, with instantaneous velocity $r^{-1/3}$, where r is that point’s radius of curvature at that time. See Figure 1.

The ACSF was first studied by Alvarez et al. [4] and Sapiro and Tannenbaum [31]. It differs from the more usual *curve-shortening flow* (CSF) [12, 16], in which each point is given instantaneous velocity r^{-1} .

Unlike the CSF, the ACSF is invariant under affine transformations: Applying an affine transformation to a curve, and then performing the ACSF, gives the same results (after rescaling the time parameter appropriately) as performing the ACSF and then applying the affine transformation to the shortened curves. Moreover, if the affine transformation preserves area, then the time scale is unaffected.

The ACSF was originally applied in computer vision, as a way of smoothing object boundaries [12] and of computing shape descriptors that are insensitive to the distortions caused by changes of viewpoint.

Properties of the CSF and ACSF for simple curves. Under either the CSF or the ACSF, a simple curve remains simple, and its length decreases strictly with time ([16], [31], resp.). Furthermore, a pair of disjoint curves, run simultaneously, remain disjoint at all times ([32], [6], resp.). More generally, the number of intersections between two curves never increases ([5], [6], resp.).

Given a smooth closed curve $\gamma : [0, 1] \rightarrow \mathbb{R}^2$, let $\alpha(s) \in \mathbb{S}^1$ be the unit vector tangent to $\gamma(s)$ for each $s \in [0, 1]$. Then the *total absolute curvature* of γ is the total distance traversed by $\alpha(s)$ in \mathbb{S}^1 as s goes from 0 to 1. If γ is convex then its total absolute curvature is exactly 2π ; otherwise, it is larger than 2π . Under either the CSF or the ACSF, the total absolute curvature of a curve

decreases strictly with time and tends to 2π ([23, 24], [6], resp.). Moreover, the number of inflection points of a simple curve does not increase with time ([5], [6], resp.).

Under the CSF, a simple curve eventually becomes convex and then converges to a circle as it collapses to a point [23, 24]. Correspondingly, under the ACSF, a simple curve becomes convex and then converges to an ellipse as it collapses to a point [6].

Self-intersecting curves. When the initial curve is not simple, a self-intersection might collapse and form a cusp with infinite curvature. For the CSF, it has been shown that, as long as the initial curve satisfies some natural conditions, it is possible with some care to define the flow past the singularity [3, 5]. Angenent [5] generalized these results to a wide range of flows, but unfortunately the ACSF is not included in this range [6]. Hence, no rigorous results have been obtained for self-intersecting curves under the ACSF. Still, ACSF computer simulations can be run on curves that have self-intersections or singularities with little difficulty.

1.3 Relation to the convex-layer decomposition

Let P be a finite set of points in the plane. The *convex-layer decomposition* (also called the *onion decomposition*) of P is the partition of P into sets P_1, P_2, P_3, \dots obtained as follows: Let $Q_0 = P$. Then, for each $i \geq 1$ for which $Q_{i-1} \neq \emptyset$, let P_i be the set of vertices of the convex hull of Q_{i-1} , and let $Q_i = Q_{i-1} \setminus P_i$. In other words, we repeatedly remove from P the set of vertices of its convex hull. See [7, 15, 18, 19].

Eppstein et al. [21], following Har-Peled and Lidický [26], studied *grid peeling*, which is the convex-layer decomposition of subsets of the integer grid \mathbb{Z}^2 . Eppstein et al. found an experimental connection between ACSF for convex curves and grid peeling. Specifically, let γ be a fixed convex curve. Let n be large, let $(\mathbb{Z}/n)^2$ be the uniform grid with spacing $1/n$, and let $P_n(\gamma)$ be the set of points of $(\mathbb{Z}/n)^2$ that are contained in the region bounded by γ . Then, as $n \rightarrow \infty$, the convex-layer decomposition of $P_n(\gamma)$ seems experimentally to converge to the ACSF evolution of γ , after the time scale is adjusted appropriately. They formulated this connection precisely in the form of a conjecture. They also raised the question whether there is a way to generalize the grid peeling process so as to approximate ACSF for non-convex curves as well.

Dalal [18] studied the convex-layer decomposition of point sets chosen uniformly and independently at random from a fixed convex domain, in the plane as well as in \mathbb{R}^d . Recently, Calder and Smart [11] proved that the above-described correspondence between ACSF and the convex-layer decomposition holds if, instead of a uniform grid, one uses a random point set sampled uniformly and independently within the region bounded by the convex curve γ .

1.4 Our Contribution

In this paper we describe a generalization of the convex-layer decomposition to non-convex, and even non-simple, curves. We call our process *homotopic curve shortening*, or HCS. Under HCS, an initial curve evolves in discrete steps in the presence of point obstacles. We find that, if the obstacles form a uniform grid, then HCS shares the same experimental connection to ACSF that grid peeling does. Hence, HCS is the desired generalization sought by Eppstein et al. [21]. We also find that the same experimental connection between ACSF and HCS (and in particular, between ACSF and the convex-layer decomposition) holds when the obstacles are distributed uniformly at random, with the sole difference being in the constant of proportionality.

Although the experimental connection between HCS and ACSF seems hard to prove, we do prove that HCS satisfies some simple properties analogous to those of ACSF: HCS is invariant

under affine transformations, preserves convexity, and does not increase the total absolute curvature. Furthermore, the number of self-intersections of a curve, or intersections between two curves (appropriately defined), does not increase. Finally, if the initial curve is simple, then the number of inflection points (appropriately defined) does not increase.

Organization of This Paper. In Section 2 we describe homotopic curve shortening (HCS), our generalization of the convex-layer decomposition. In Section 3 we present our conjectured connection between ACSF and HCS, as well as experimental evidence supporting this connection. In Section 4 we state our theoretical results, to the effect that HCS satisfies some properties analogous to those of ACSF. In Section 5 we prove the results stated in Section 4. Appendices A–C include proofs of some known results for the sake of completeness, as well as implementation details of our experiments.

2 Homotopic curve shortening

Let P be a finite set of obstacle points. A P -curve (resp. P -path) is a curve (resp. path) that is composed of straight-line segments, where each segment starts and ends at obstacle points.

Homotopic curve shortening (HCS) is a discrete process that starts with an initial P -curve γ_0 (which might self-intersect), and at each step, the current P -curve γ_n is turned into a new P -curve $\gamma_{n+1} = \text{HCS}_P(\gamma_n)$.

The definition of $\gamma' = \text{HCS}_P(\gamma)$ for a given P -curve γ is as follows. Let (p_0, \dots, p_{m-1}) be the circular list of obstacle points visited by γ . Call p_i *nailed* if γ goes straight through p_i , i.e. if $\angle p_{i-1}p_i p_{i+1} = \pi$.¹ Let (q_0, \dots, q_{k-1}) be the circular list of nailed vertices of γ . Suppose first that $k \geq 1$. Then γ' is obtained through the following three substeps:

1. *Splitting.* We split γ into k P -paths $\delta_0, \dots, \delta_{k-1}$ at the nailed vertices, where each δ_i goes from q_i to q_{i+1} .
2. *Shortcutting.* For each non-endpoint vertex p_i of each δ_i , we make the curve avoid p_i by taking a small shortcut. Specifically, let $\varepsilon > 0$ be sufficiently small, and for each i let C_{p_i} be a circle of radius ε centered at p_i . Let e_i be the segment $p_{i-1}p_i$ of δ_i . Let $x_i = e_i \cap C_{p_i}$ and $y_i = e_{i+1} \cap C_{p_i}$. Then we make the path go straight from x_i to y_i instead of through p_i . Call the resulting path ρ_i , and let ρ be the curve obtained by concatenating all the paths ρ_i .
3. *Shortening.* Each ρ_i in ρ is replaced by the shortest P -path homotopic to it. The resulting curve is γ' .

If γ has no nailed vertices ($k = 0$) then γ' is obtained by performing the shortcutting and shortening steps on the single closed curve γ . Note that if P is in general position (no three points on a line) then there will never be nailed vertices. Figure 2 illustrates one HCS step on a sample curve.

The process terminates when the curve collapses to a point. This will certainly happen after a finite number of steps, since at each step the curve gets strictly shorter, and there is a finite number of distinct P -curves of at most a certain length.

HCS for convex curves. If the initial curve γ_0 is the boundary of the convex hull of P , then the HCS evolution of γ_0 is equivalent to the convex-layer decomposition of P . Namely, for every $i \geq 0$, the curve γ_i is the boundary of a convex polygon, and the set of vertices of this polygon equals the $(i + 1)$ -st convex layer of P . See Section 4 below.

¹All indices in circular sequences are modulo the length of the sequence.

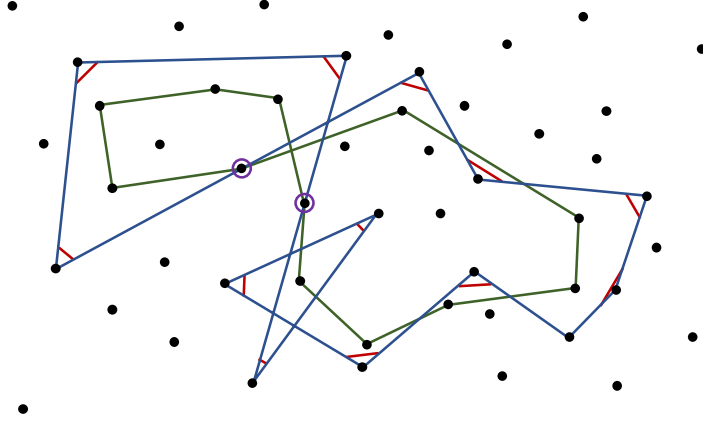


Figure 2: Computation of a single step of homotopic curve shortening: Given a P -curve γ (blue), we first identify its nailed vertices (purple). In this case, the two nailed vertices split γ into two paths δ_0, δ_1 . In each δ_i we take a small shortcut around each intermediate vertex (red). Then we replace each δ_i by the shortest path homotopic to it, obtaining the new P -curve $\gamma' = \text{HCS}_P(\gamma)$ (green).

3 Experimental connection between ACSF and HCS

Our experiments show that HCS, using $P = (\mathbb{Z}/n)^2$ as the obstacle set, approximates ACSF at the limit as $n \rightarrow \infty$, just as grid peeling approximates ACSF for convex curves. The connection between the two processes is formalized in the following conjecture, which generalizes Conjecture 1 of [21].

Conjecture 1. *There exists a constant $c_g \approx 1.6$ such that the following is true: Let δ be an initial curve. Fix a time $t > 0$ for which $\delta' = \delta(t)$ under ACSF is defined. For a fixed n , let γ_0 be the shortest curve homotopic to δ under obstacle set $P_n = (\mathbb{Z}/n)^2$. Let $m = \lfloor c_g t n^{4/3} \rfloor$, and let $\gamma_m = \text{HCS}_P^{(m)}(\gamma_0)$ be the result of m iterations of HCS starting with γ_0 . Then, as $n \rightarrow \infty$, the Fréchet distance between γ_m and δ' tends to 0.*

Furthermore, we find that the connection between ACSF and HCS also holds if the uniform grid $(\mathbb{Z}/n)^2$ is replaced by a random point set, though with a different constant of time proportionality.

Conjecture 2. *There exists a constant $c_r \approx 1.3$ such that the following is true: Let δ be an initial curve, contained in a convex region R of area A . Fix a time $t > 0$ for which $\delta' = \delta(t)$ under ACSF is defined. For a fixed n , let P be a set of An^2 obstacle points chosen uniformly and independently at random from R . Let γ_0 be the shortest curve homotopic to δ under obstacle set P . Let $m = \lfloor c_r t n^{4/3} \rfloor$, and let $\gamma_m = \text{HCS}_P^{(m)}(\gamma_0)$ be the result of m iterations of HCS starting with γ_0 . Then, as $n \rightarrow \infty$, the Fréchet distance between γ_m and δ' is almost surely smaller than ε , for some $\varepsilon = \varepsilon(n)$ that tends to 0 with n .*

As mentioned above, Conjecture 2 was recently proven by Calder and Smart [11] for the special case where δ is a convex curve. Furthermore, they point out that their experiments seem to suggest $c_r = 4/3$.

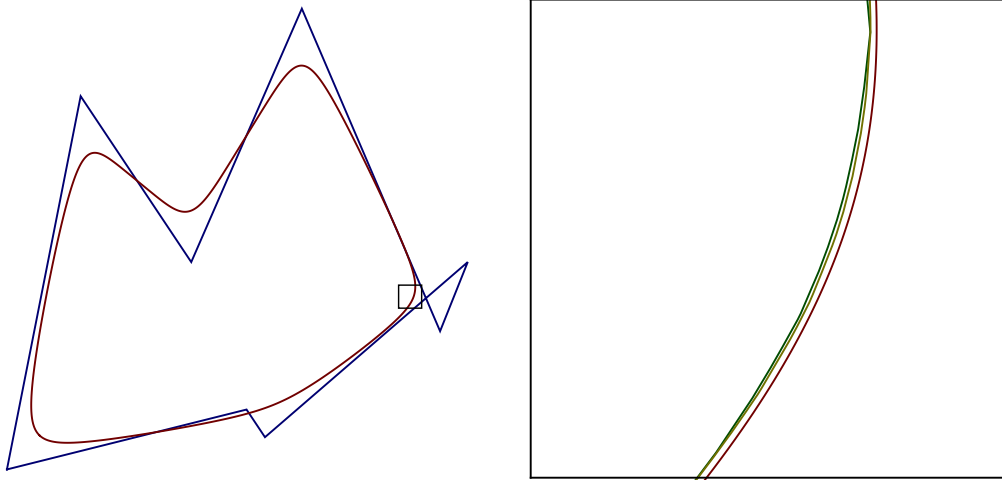


Figure 3: Left: Initial curve Δ (blue) and simulated ACSF result after the curve's length reduced to 70% of its original length (red). Right: Comparison between ACSF approximation (red), HCS with $n = 10^7$ uniform-grid obstacles (green), and HCS with $n = 10^7$ random obstacles (yellow) on a small portion of the curve.

3.1 Experiments

We tested Conjectures 1 and 2 on a variety of test curves. We found that for all our test curves, the result of HCS does seem to converge to the result of ACSF as $n \rightarrow \infty$, both for grid and for random obstacle sets.

Let us illustrate our experiments on the piecewise-linear curve Δ having vertices $(0, 0)$, $(0.16, 0.81)$, $(0.4, 0.45)$, $(0.64, 1)$, $(0.94, 0.3)$, $(1, 0.45)$, $(0.56, 0.07)$, $(0.52, 0.13)$. We approximated ACSF using an approach similar to the one in [21]. We ran our ACSF simulation on Δ until we obtained a curve Δ' whose length equals 70% of the original length of Δ . See Figure 3 (left). This happened at $t^* \approx 0.0266$. By this time, the self-intersection and an inflection point of the curve have disappeared.

Then we introduced in the unit square $[0, 1]^2 \supset \Delta$ a set P of n obstacle points, where P is either a uniform grid (i.e. a $\sqrt{n} \times \sqrt{n}$ grid) G_n , or a random set R_n . For each case, we initially snapped each vertex of Δ to its closest point in P , obtaining a P -curve, and then we ran HCS until the length of the curve shrank to 70% of its original length, obtaining a new curve $\Delta'' = \Delta''(P)$. We did this for several values of n . For each case, we computed $h(\Delta', \Delta'')$, where $h(\gamma_1, \gamma_2)$ for piecewise-linear curves γ_1, γ_2 is defined as the maximum distance between a vertex of one curve and the closest point on the other curve. (For “nice” curves as ours, there is no significant difference, if at all, between this distance h and either the Hausdorff or the Fréchet distance between the two curves.)

For random obstacles, we conducted this experiment for $n = 10^4, 10^5, 10^6, 10^7$, taking the average of 5 samples for each value of n . Our random-obstacle program is limited by memory rather than by time, since it stores all the obstacle points in memory. For uniform-grid obstacles, we conducted this experiment also for $n = 10^8$. After this point, our ACSF approximation Δ' does not seem to be accurate enough for reliable comparisons. The results are shown in Figure 4 (left).

We also checked whether the relation between the ACSF time t^* and the number of HCS iterations m behaves as predicted by Conjectures 1 and 2. For this purpose, we computed $c = m/(t^*n^{2/3})$ for each case, and checked whether c is roughly constant. The results are shown in Table 1.

As we can see, Conjectures 1 and 2 are well supported by the experiments.

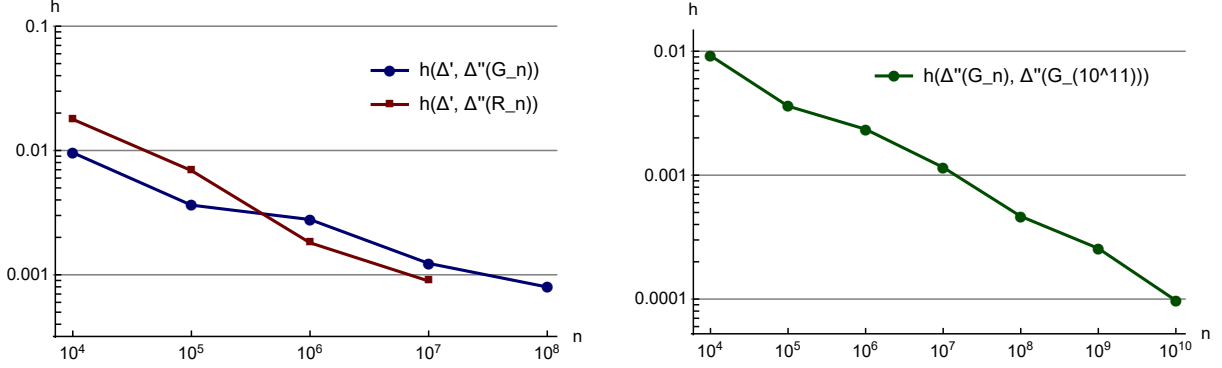


Figure 4: Left: Distance between ACSF approximation and HCS with uniform-grid obstacles (blue curve) or random obstacles (red curve, average of 5 trials), for increasing values of n , the number of obstacles. Right: Distance between HCS with uniform-grid obstacles for $n = 10^4, \dots, 10^{10}$ and with $n = 10^{11}$.

n	iterations with G_n	c_g	avg. iterations with R_n	c_r
10^4	20	1.616	15.6	1.261
10^5	93	1.619	75.2	1.309
10^6	434	1.628	351.2	1.317
10^7	2006	1.621	1628.6	1.316
10^8	9266	1.613		

Table 1: Approximations of the constants c_g and c_r given by the experiments.

Finally, we measured the rate of convergence of the uniform-grid HCS to its limit shape as $n \rightarrow \infty$. To this end, we computed $h(\Delta''(G_n), \Delta''(G_m))$ for $n \in \{10^4, 10^5, \dots, 10^{10}\}$ and $m = 10^{11}$. See Figure 4 (right). As we can see, increasing n by a factor of 10 has the effect of multiplying the distance by roughly a factor of 0.47.

See Appendix C for some implementation details of our ACSF and HCS simulations.

4 Properties of homotopic curve shortening

In this paper we prove that HCS satisfies some properties analogous to those of ACSF. This section contains the statements of our results, and the proofs appear in Section 5.

Lemma 3. *HCS is invariant under affine transformations. Namely, if P is a set of obstacle points, γ is a P -curve, and T is a non-degenerate affine transformation, then $T(\text{HCS}_P(\gamma)) = \text{HCS}_{T(P)}(T(\gamma))$.*

In particular, if T is a grid-preserving affine transformation, meaning that T maps $(\mathbb{Z}/n)^2$ injectively to itself, then the HCS evolution using $P = (\mathbb{Z}/n)^2$ (as in Conjecture 1) is unaffected by T . Hence, HCS on uniform-grid obstacles is invariant under a certain subset of the area-preserving affine transformations, just as in grid peeling [21].

Also, if T is an area-preserving affine transformation, then the probability distribution of random sets P in the convex region R of Conjecture 2 stays unaffected after applying T to R .

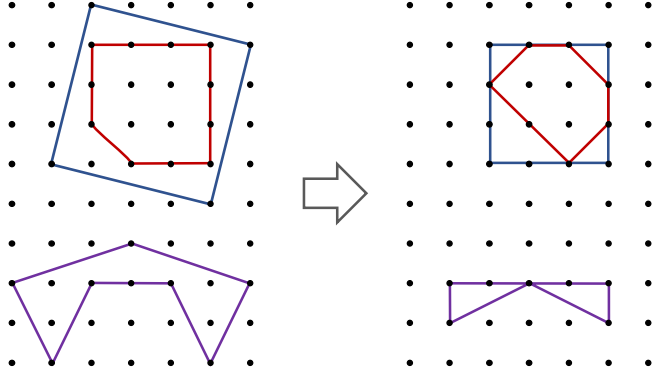


Figure 5: HCS might cause disjoint curves to intersect, or a simple curve to self-intersect.

Lemma 4. *Let γ be a simple P -curve, and let $\gamma' = \text{HCS}_P(\gamma)$. If γ is the boundary of a convex polygon, then so is γ' . Hence, under HCS, once a curve becomes the boundary of a convex polygon, it stays that way.*

The *total absolute curvature* of a piecewise-linear curve γ with vertices (p_0, \dots, p_{m-1}) is the sum of the exterior angles $\sum_{i=0}^{m-1} (\pi - |\angle p_{i-1} p_i p_{i+1}|)$. It equals 2π if γ is the boundary of a convex polygon, and it is larger than 2π otherwise.

Lemma 5. *Let γ be a P -curve, and let $\gamma' = \text{HCS}_P(\gamma)$. Let α, α' be the total absolute curvature of γ, γ' , respectively. Then $\alpha \geq \alpha'$. Hence, under HCS, the total absolute curvature of a curve never increases.*

If γ, δ are disjoint P -curves, then $\text{HCS}_P(\gamma), \text{HCS}_P(\delta)$ are not necessarily disjoint. Similarly, if γ is a simple P -curve, then $\text{HCS}_P(\gamma)$ is not necessarily simple. See Figure 5.

Curves γ, δ are called *disjoinable* if they can be made into disjoint curves by performing on them an arbitrarily small perturbation. Similarly, a curve γ is called *self-disjoinable* if it can be turned into a simple curve by an arbitrarily small perturbation. Note that if γ is self-disjoinable then γ, γ are disjoinable, though the reverse is not necessarily true: Consider for example a curve γ that makes two complete clockwise turns around the unit circle.

A self-disjoinable curve is also called *weakly simple*. Akitaya et al. [1] recently found an algorithm for recognizing weakly simple polygons in time $O(n \log n)$. (See also [2] for an $O(n \log n)$ -time algorithm for the more general problem of recognizing *weak-embeddings* of graphs.)

An intersection between two curves, or between two portions of one curve, is called *transversal*, if at the point of intersection both curves are differentiable and their normal vectors are not parallel at that point. If all intersections between curves γ_1 and γ_2 are transversal, then we say that γ_1, γ_2 are themselves *transversal*. Similarly, if all self-intersections of γ are transversal, then we say that γ is *self-transversal*. (Transversal and self-transversal curves are sometimes called *generic*, see e.g. [13].)

If γ is self-transversal, we denote by $\chi(\gamma)$ the number of self-intersections of γ .² If γ is not self-transversal, then we define $\chi(\gamma)$ as the minimum of $\chi(\hat{\gamma})$ among all self-transversal curves $\hat{\gamma}$ that are ε -close to γ , for all small enough $\varepsilon > 0$. Hence, $\chi(\gamma) = 0$ if and only if γ is self-disjoinable. We define similarly the number of intersections $\chi(\gamma_1, \gamma_2)$ between two curves. Then, γ_1 and γ_2

²A self-intersection in a curve $\gamma : \mathbb{S}^1 \rightarrow \mathbb{R}^2$ is a pair $s \neq t$ such that $\gamma(s) = \gamma(t)$. Hence, if γ passes k times through a certain point, that counts as $\binom{k}{2}$ self-intersections.

are disjoint if and only if $\chi(\gamma_1, \gamma_2) = 0$. Fulek and Tóth recently proved that the problem of computing $\chi(\gamma)$ is NP-hard [22].

Theorem 6. *Let γ be a P -curve, and let $\gamma' = \text{HCS}_P(\gamma)$. Then their self-intersection numbers satisfy $\chi(\gamma') \leq \chi(\gamma)$. Let δ be another P -curve, and let $\delta' = \text{HCS}_P(\delta)$. Then their intersection numbers satisfy $\chi(\gamma', \delta') \leq \chi(\gamma, \delta)$. In particular, if γ is self-disjoinable, so is γ' , and if γ, δ are disjoint, then so are γ', δ' . Hence, under HCS, the intersection and self-intersection numbers never increase.*

With the technique of Theorem 6 we can obtain an upper bound on the number of iterations of HCS:

Theorem 7. *For a fixed obstacle set P , the P -curve γ that maximizes the number of HCS iterations is the boundary of the convex hull of P .*

As mentioned above, if γ is the boundary of the convex hull of P , then the HCS process starting with γ is just the convex-layer decomposition of P . Hence, by Theorem 7, if $|P| = n$ then the HCS process starting with any P -curve ends in at most $n/2$ iterations. If $P = \{1, 2, \dots, \sqrt{n}\}^2$ then the process ends in at most $O(n^{2/3})$ iterations (by Har-Peled and Lidický [26]). And if P is uniformly and independently chosen at random inside a fixed convex domain, then the expected number of iterations is $O(n^{2/3})$ (by Dalal [18]).

Recall that an obstacle set P is in general position if no three points of P lie on a line; and recall that if P is in general position then there are no nailed vertices in HCS.

Theorem 8. *Let P be an obstacle set in general position. Let γ be a simple P -curve. Then $\text{HCS}_P(\gamma)$ is also simple. Let γ_1, γ_2 be disjoint P -curves. Then $\text{HCS}_P(\gamma_1), \text{HCS}_P(\gamma_2)$ are also disjoint. Hence, under HCS with obstacles in general position, a simple curve stays simple, and a pair of disjoint curves stay disjoint.*

Let γ be a simple piecewise-linear curve with vertices (v_0, \dots, v_{n-1}) . Assume that the sequence of vertices is minimal, meaning no v_{i-1}, v_i, v_{i+1} lie on a straight line. An *inflection edge* of γ is an edge $v_i v_{i+1}$ such that the previous and next vertices v_{i-1}, v_{i+2} lie on opposite sides of the line through v_i, v_{i+1} . Let $\iota(\gamma)$ be the number of inflection edges of γ . Note that $\iota(\gamma)$ is always even, since every inflection edge lies either after a sequence of clockwise vertices and before a sequence of counterclockwise vertices, or vice versa.

If γ is not simple but self-disjoinable, then we define $\iota(\gamma)$ as the minimum of $\iota(\gamma')$ over all simple piecewise-linear curves γ' that are ε -close to γ , for all sufficiently small $\varepsilon > 0$. (Note that for a given γ there might exist different curves γ' with different values of $\iota(\gamma')$. For example, if γ goes from a point p to a point q and back n times, then γ' could be a spiral with just two inflection edges, or a double zig-zag with $2n - 2$ inflection edges.)

Theorem 9. *Let γ be self-disjoinable, and let $\gamma' = \text{HCS}_P(\gamma)$. Then their inflection-edge numbers satisfy $\iota(\gamma') \leq \iota(\gamma)$. Hence, under HCS on a self-disjoinable curve, the curve's number of inflection edges never increases.*

5 Proofs

In order to prove the properties stated in Section 4, we rely on two different approaches for computing shortest homotopic curves. The first approach is the one given by [14, 28, 29, 30], which uses a triangulation of the ambient space. The second approach consists of repeatedly releasing unstable vertices. We start by describing these two approaches in detail.

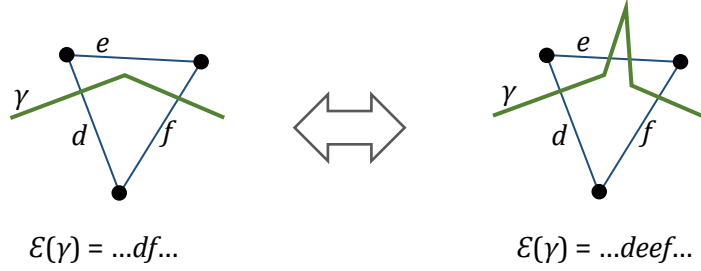


Figure 6: Combinatorial changes in the edge sequence of a continuously changing curve γ .

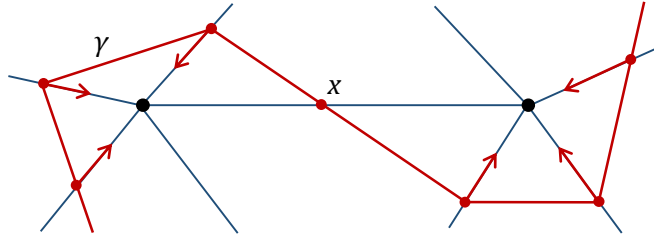


Figure 7: In the shortest curve homotopic to γ , the position of the point x is not uniquely defined.

For simplicity, we restrict ourselves to piecewise-linear curves. By the relative simplicial approximation theorem (Zeeman [33]), we can restrict ourselves to piecewise-linear homotopies as well.

5.1 Triangulations

Let P be a finite set of point obstacles, and let γ be a piecewise-linear curve avoiding P . Assume without loss of generality that γ is contained in the convex hull of P (by adding points outside the convex hull of γ if necessary). Let \mathcal{T} be a triangulation of the convex hull of P using the points of P as vertices.

We can assume without loss of generality that the curve γ intersects each triangle edge transversally. Let $\mathcal{E} = \mathcal{E}(\gamma)$ be the circular sequence of triangle edges intersected by γ . Then a piecewise-linear homotopic change of γ can only have two possible types of effects on \mathcal{E} : Either an adjacent pair ee is inserted somewhere in the sequence, or an existing such pair is deleted. See Figure 6. Hence, two curves γ, γ' are homotopic if and only if their corresponding edge sequences $\mathcal{E}(\gamma), \mathcal{E}(\gamma')$ are *equivalent*, in the sense that they can be transformed into one another by a sequence of operations of these two types.

Call an edge sequence $\mathcal{E}(\gamma)$ *reduced* if it contains no adjacent pair ee . Then every edge sequence is equivalent to a unique reduced sequence. (Proof sketch: Supposing for a contradiction that there exist two distinct equivalent reduced sequences S_1, S_2 , consider a transformation of S_1 into S_2 that uses the minimum possible number of deletions, and among those, consider one in which the first deletion is done as early as possible. Then it is easy to arrive at a contradiction.)

Hence, in order to compute the shortest curve homotopic to γ , we first compute $\mathcal{E}(\gamma)$, then we reduce this sequence by repeatedly removing adjacent pairs, obtaining a reduced sequence \mathcal{E}' , then we place a point $x(e)$ on each $e \in \mathcal{E}'$, and then we slide the points $x(e)$ along their edges so as to minimize the length of the curve. This last step can be done using the “funnel algorithm” (see [14, 28, 29, 30]); we omit the details.

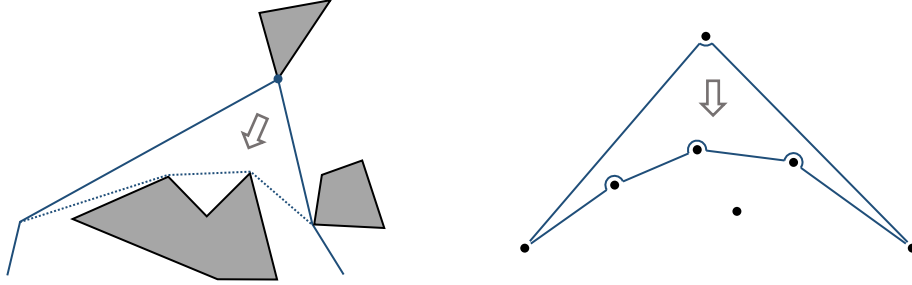


Figure 8: Releasing an unstable vertex in the presence of polygonal obstacles (left) or point obstacles (right).

For the sake of completeness, we include in Appendix A a proof that there is always a unique shortest curve. Note that, even though the shortest curve is always unique, the final positions of the points $x(e)$ are not necessarily unique. This can happen if a triangulation edge is an edge of the final curve. See Figure 7.

5.2 The vertex release algorithm

We now present another simple algorithm for the shortest homotopic curve problem. This algorithm is not mentioned in any previous publication that we are aware of, but it is similar in spirit to well-known algorithms, in particular to the funnel algorithm.

As a warm-up, let us first consider the case in which the obstacles are not single points but rather polygons. Let γ be a piecewise-linear curve that avoids the interior of all the obstacles. Call a vertex $v = \gamma(t_i)$ of γ *unstable* if v does not lie on any obstacle, or if v lies on the boundary of an obstacle T , but T lies locally on the side of γ at which the angle is larger than π . If v is unstable, then the process of *releasing* v is as follows: Let $u = \gamma(t_{i-1})$ and $w = \gamma(t_{i+1})$ be the previous and next vertices of γ . Suppose first that $u \neq w$. Let Δ be the triangle uvw , and let S be the set of obstacle vertices that lie inside Δ . Let u, z_1, \dots, z_k, w be the vertices of the convex hull of $S \setminus \{v\}$ in order. Then we replace v by z_1, \dots, z_k in γ . The new vertices z_1, \dots, z_k are necessarily stable, but u and w might change from stable to unstable or vice versa. If $u = w$ then we simply remove v and w from γ . See Figure 8 (left).

Then the algorithm consists of releasing unstable vertices one by one, in an arbitrary order, until no more unstable vertices remain.

If there are also point obstacles, then the algorithm becomes slightly more complicated. For each curve vertex $v = \gamma(t_i)$ that lies on a point obstacle, we need to remember the corresponding signed angle α_i that the curve turns around the obstacle, since this angle could be larger than 2π in absolute value. The angle α_i is always congruent modulo 2π to $\angle uvw$, where $u = \gamma(t_{i-1})$ and $w = \gamma(t_{i+1})$ are the previous and next vertices. The vertex v is unstable if and only if $|\alpha_i| < \pi$.

If v is unstable, then in order to release it we proceed as described above, and we update the angles as follows (see Figure 8, right):

- If $u \neq w$ then we give to each new vertex z_j the unique appropriate angle β_j that has the opposite sign of α_i and satisfies $\pi \leq |\beta_j| < 2\pi$. We then update the angles α_{i-1} and α_{i+1} at u and w as follows: Denote $z_0 = u$ and $z_{k+1} = w$ (in order to handle properly the case $k = 0$). We add to α_{i-1} the angle $\angle vuz_1$, and we add to α_{i+1} the angle $\angle z_k wv$.
- If $u = w$ then we update α_{i-1} by adding to it the angle α_{i+1} .

Lemma 10. *The vertex release algorithm always finds the shortest curve δ homotopic to the given piecewise-linear curve γ , irrespective of the order of release of the vertices.*

Proof. The vertex-release algorithm ends in a finite number of iterations, since at each iteration the length of the curve strictly decreases and the number of vertices not touching obstacles never increases. Hence, there exists a finite number of distinct possible curves the algorithm might go through.

The final curve δ is clearly homotopic to the initial curve γ . Moreover, the final curve is locally shortest, in the sense that for every sufficiently small $\varepsilon > 0$, every other curve δ' homotopic to γ and ε -close to δ is longer than δ . But in the Euclidean plane with polygonal or point obstacles, for every curve there exists a unique locally shortest curve homotopic to it. (For completeness, we include the proof of this fact in Appendix A.) Hence, δ is indeed the shortest curve homotopic to γ . \square

5.3 Proof of Lemmas 3–5

Lemmas 3–5 follow easily from the vertex-release algorithm (Lemma 10).

Lemma 3. *HCS is invariant under affine transformations. Namely, if P is a set of obstacle points, γ is a P -curve, and T is a non-degenerate affine transformation, then $T(\text{HCS}_P(\gamma)) = \text{HCS}_{T(P)}(T(\gamma))$.*

Proof. The claim follows from the fact that shortest homotopic curves and paths are invariant under affine transformations. Namely, let γ be a curve or path in the presence of obstacle points P , let δ be the shortest curve or path homotopic to γ , and let $T : \mathbb{R}^2 \rightarrow \mathbb{R}^2$ be a non-degenerate affine transformation. Then the shortest curve or path homotopic to $T(\gamma)$ in the presence of $T(P)$ is $T(\delta)$. This, in turn, follows from the fact that T does not affect whether a vertex is stable or unstable, and furthermore, if a vertex is unstable, then it does not matter whether we first release the vertex and then apply T , or do these operations in the opposite order. \square

Lemma 4. *Let γ be a simple P -curve, and let $\gamma' = \text{HCS}_P(\gamma)$. If γ is the boundary of a convex polygon, then so is γ' . Hence, under HCS, once a curve becomes the boundary of a convex polygon, it stays that way.*

Proof. This follows from the fact that the property of being the boundary of a convex polygon is preserved by each vertex release. \square

Lemma 5. *Let γ be a P -curve, and let $\gamma' = \text{HCS}_P(\gamma)$. Let α, α' be the total absolute curvature of γ, γ' , respectively. Then $\alpha \geq \alpha'$. Hence, under HCS, the total absolute curvature of a curve never increases.*

Proof. Given a piecewise-linear curve γ with vertices (p_0, \dots, p_{m-1}) , let $v_i \in \mathbb{S}^1$ be the unit vector parallel to $\overrightarrow{p_i p_{i+1}}$ for each i . Call a tour of \mathbb{S}^1 *valid* if it visits the vectors $v_0, v_1, \dots, v_{m-1}, v_0$ in this order. Then the total absolute curvature of γ equals the length of the shortest valid tour of \mathbb{S}^1 .

Now let γ be a given P -curve, and let $\gamma' = \text{HCS}_P(\gamma)$. Recall that γ' is obtained from γ by a series of vertex releases. Each vertex release replaces two adjacent vectors $v_i, v_{i+1} \in \mathbb{S}^1$ by a certain number $k \geq 1$ of vectors w_1, \dots, w_k lying between them, in this order. Hence, the shortest valid tour of \mathbb{S}^1 for the old vector sequence goes from v_i to v_{i+1} through w_1, \dots, w_k , and hence this tour is also valid for the new vector sequence. \square

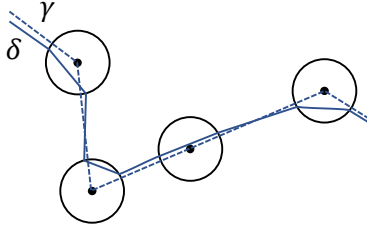


Figure 9: A P -curve γ and a corresponding type-2 curve δ .

5.4 Proof of Theorems 6–8

The proof of Theorems 6–8 is based on the triangulation technique. Let γ be a P -curve, let $\varepsilon > 0$ be small enough, and let $\hat{\gamma}$ be a self-transversal curve that is ε -close to γ and has the minimum possible number of self-intersections. In order to prove Theorem 6 regarding intersection and self-intersection numbers, we proceed as follows:

1. We show that, without loss of generality, we can assume that $\hat{\gamma}$ passes through the “correct side” of each non-nailed obstacle, as in the “shortcutting” step of HCS.
2. We modify $\hat{\gamma}$ homotopically, by first eliminating repetitions in its edge sequence \mathcal{E} and then sliding its vertices along the triangulation edges, until each vertex comes within ε of its final position as given by $\gamma' = \text{HCS}_P(\gamma)$. We show that the number of self-intersections never increases in the process.

The case of two curves is similar.

In order to do the first step, we define a type of curves that are ε -close to P -curves and pass through the “correct side” of non-nailed obstacles. We call them *type-2 curves*. We also define a “snapping” operation, which transforms $\hat{\gamma}$ into a type-2 curve without increasing its number of self-intersections.

Type-2 curves. Let γ be a P -curve, let (p_0, \dots, p_{k-1}) be the circular list of obstacles visited by γ , and let $\varepsilon > 0$ be small enough. For each $p \in P$, let C_p be a circle of radius ε centered at p . For each i , let $x_i \in C_{p_i}$ be a point at distance at most ε^2 from the segment $p_{i-1}p_i$, and let $y_i \in C_{p_i}$ be a point at distance at most ε^2 from the segment $p_i p_{i+1}$. Then a type-2 curve δ corresponding to γ travels in a straight line from y_{i-1} to x_i and then in a straight line from x_i to y_i for each i . See Figure 9. We call each segment $y_{i-1}x_i$ a *long part* and each segment $x_i y_i$ a *short part*. If $\angle p_{i-1}p_i p_{i+1} \neq \pi$ and ε is chosen small enough, then p_i lies on the side of the curve at which the angle is larger than π . If $\angle p_{i-1}p_i p_{i+1} = \pi$ then the corresponding short part passes within distance ε^2 of v_i .

The snapping operation. Let γ be a P -curve, and let $\hat{\gamma}$ be a curve (ε^2)-close to γ . We define the type-2 curve $\text{snap}(\hat{\gamma})$ as follows. For each p_i visited by $\hat{\gamma}$ there exists a point z_i in $\hat{\gamma}$ that is within distance ε^2 of p_i . Let y_i be the first intersection of $\hat{\gamma}$ with C_{p_i} that comes after z_i , and let x_i be the last intersection of $\hat{\gamma}$ with C_{p_i} that comes before z_i . (Thus, the part of $\hat{\gamma}$ between x_i and y_i is entirely contained in the disk bounded by C_{p_i} .) Then we let $\text{snap}(\hat{\gamma})$ be the type-2 curve that uses these points x_i, y_i for all i as vertices.

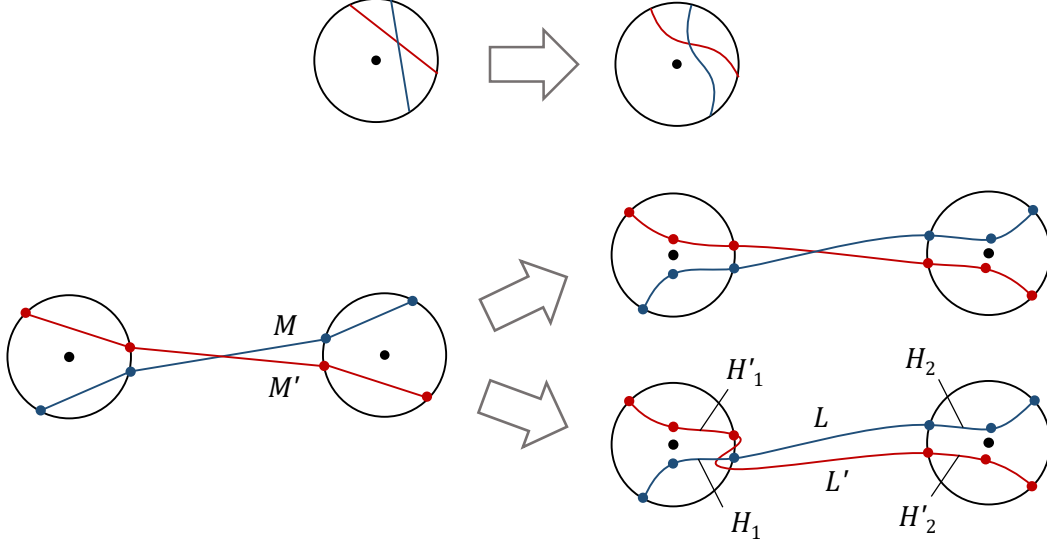


Figure 10: Each self-intersection of δ can be traced back to a self-intersection of $\hat{\gamma}$. Different portions of δ and $\hat{\gamma}$ are shown in different colors.

Lemma 11. *Let γ be a P -curve, and let $\hat{\gamma}$ be a self-transversal curve (ε^2) -close to γ , such that no self-intersection of $\hat{\gamma}$ occurs on any circle C_p . Then the curve $\delta = \text{snap}(\hat{\gamma})$ also is self-transversal, and it satisfies $\chi(\delta) \leq \chi(\hat{\gamma})$.*

Similarly, let γ_1, γ_2 be P -curves, and let $\hat{\gamma}_1, \hat{\gamma}_2$ be transversal curves (ε^2) -close to them, respectively, such that no intersection between $\hat{\gamma}_1$ and $\hat{\gamma}_2$ occurs on any circle C_p . Then the curves $\delta_1 = \text{snap}(\hat{\gamma}_1), \delta_2 = \text{snap}(\hat{\gamma}_2)$ are transversal and satisfy $\chi(\delta_1, \delta_2) \leq \chi(\hat{\gamma}_1, \hat{\gamma}_2)$.

Proof. We will show that each self-intersection of δ can be mapped to a self-intersection of $\hat{\gamma}$, such that different self-intersections of δ are mapped to different self-intersections of $\hat{\gamma}$.

The points x_i, y_i define a partition of $\hat{\gamma}$ into *long* and *short parts* corresponding to the long and short parts of δ . On each short part of $\hat{\gamma}$ inside a circle C_{p_i} , pick a point z_i that is at distance at most $2\varepsilon^2$ from p_i , and such that $\hat{\gamma}$ passes through z_i only once. Each point z_i partitions its short part into two *half-short parts*.

Now, suppose two short parts of δ within the same circle C_{p_i} intersect. Then the two corresponding short parts of $\hat{\gamma}$ must also intersect. See Figure 10 (top).

Next, suppose two long parts of δ intersect. Then either they connect two different pairs of circles, or they both connect a circle C_p to a circle C_q . In the first case, trivially the two corresponding long parts of $\hat{\gamma}$ also intersect. In the second case, if the two corresponding long parts of $\hat{\gamma}$ intersect then we are done. So suppose this is not the case. We claim that in this case, one of the long parts of $\hat{\gamma}$ must intersect one of the half-short parts adjacent to the other long part. See Figure 10 (bottom).

Let L, L' be the two long parts of $\hat{\gamma}$. Let H_1, H_2 be the half-short parts adjacent to L , and let H'_1, H'_2 be the half-short parts adjacent to L' . Let V be the concatenation of H_1, L, H_2 , and let V' be the concatenation of H'_1, L', H'_2 . Let M, M' be the long parts of δ corresponding to L, L' . Let W be the concatenation of H_1, M, H_2 , and let W' be the concatenation of H'_1, M', H'_2 . Since δ is $(2\varepsilon^2)$ -close to $\hat{\gamma}$, there exists a homotopy from V to W that does not pass through any endpoint of V' , and there exists a homotopy from V' to W' that does not pass through any endpoint of V . Therefore, the number of intersections between V and V' has the same parity as the number of

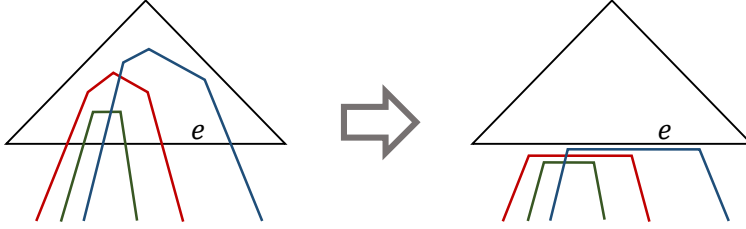


Figure 11: Reducing a curve's edge sequence without increasing its number of self-intersections. Different portions of the curve are shown in different colors.

intersections between W and W' . Since L and L' do not intersect but M and M' intersect once, a single intersection is created in the transition from V, V' to W, W' . Hence, an odd number of intersections must have been lost. These intersections must have been between a long part of one curve and a half-short part of the other curve, as claimed.

This finishes the proof that $\chi(\delta) \leq \chi(\hat{\gamma})$. A similar argument applies for the case of two curves. \square

Theorem 6. *Let γ be a P -curve, and let $\gamma' = \text{HCS}_P(\gamma)$. Then their self-intersection numbers satisfy $\chi(\gamma') \leq \chi(\gamma)$. Let δ be another P -curve, and let $\delta' = \text{HCS}_P(\delta)$. Then their intersection numbers satisfy $\chi(\gamma', \delta') \leq \chi(\gamma, \delta)$. In particular, if γ is self-disjoinable, so is γ' , and if γ, δ are disjoint, then so are γ', δ' . Hence, under HCS, the intersection and self-intersection numbers never increase.*

Proof. Let γ be a P -curve, let $\varepsilon > 0$ be small enough, and let $\hat{\gamma}$ be a self-transversal curve that is (ε^2) -close to γ and has the minimum possible number of self-intersections. Fix a triangulation \mathcal{T} of P . Assume without loss of generality that $\hat{\gamma}$ does not pass through any obstacle, and that no self-intersection of γ lies on any edge of \mathcal{T} . Let $\eta = \text{snap}(\hat{\gamma})$. Hence, η is a self-transversal curve that is ε -close to γ , passes through the “correct side” of each non-nailed obstacle, and does not have more self-intersections than $\hat{\gamma}$. Partition η into paths $\eta_0, \dots, \eta_{k-1}$ that are ε -close to the corresponding paths $\delta_0, \dots, \delta_{k-1}$ of the HCS “splitting” step, by introducing split points as follows: For each nailed visit to an obstacle $p \in P$, we choose a split point that is within distance $O(\varepsilon)$ of p and lies on a triangle edge (where the implicit constant depends only on P).

Then we modify each η_i into a homotopic path η'_i whose edge sequence $\mathcal{E}(\eta'_i)$ is reduced. We do this without increasing the number of intersections, by repeatedly doing the following: Let e be triangulation edge such that ee appears one or more times in the sequences $\mathcal{E}(\eta'_i)$. We shortcut the corresponding paths η'_i so as to not cross e at all, instead keeping a small distance from e . We make the distance to e inversely related to the distance between the two crossing points of η'_i with e . See Figure 11.

Next, we modify each η'_i into η''_i by straightening out each part within each triangle of \mathcal{T} . Hence, each η''_i is determined by the position of its vertices $x(e)$ along the triangle edges e .

Let η'' be the curve formed by concatenating the paths η''_i for all i . By appropriately sliding the non-endpoint vertices of the paths η''_i along their triangulation edges, we can bring η'' to be ε -close to γ' . However, we must be careful to perform this sliding without unnecessarily switching the order of any pair over vertices along the same edge. Meaning, whenever γ' contains several vertices along an edge that coincide, we place the corresponding vertices of η'' within ε of each other, conserving the order they had before the sliding. Let η''' be the curve obtained after sliding the vertices this way. Hence, η''' is ε -close to γ' . Table 2 summarizes the construction of the different curves.

Curve	Description
γ	Given P -curve
$\widehat{\gamma}$	Self-transversal curve (ε^2)-close to γ
η	$\text{snap}(\widehat{\gamma})$
η'	Result of reducing edge sequences of paths η_i in η
η''	Result of straightening η' within triangles of \mathcal{T}
η'''	Result of sliding vertices of η'' along \mathcal{T} -edges; ε -close to γ'
γ'	$\text{HCS}(\gamma)$

Table 2: Curves used in the proofs of Theorems 6–8.

We now claim that the number of self-intersections of η''' is not larger than that of η'' .

Let (x_0, \dots, x_{m-1}) be the circular list of vertices of η'' , and let (y_0, \dots, y_{m-1}) be the corresponding vertices of η''' , meaning that for each j , both vertices x_j, y_j lie on the same triangulation edge e_j . Consider a self-intersection z lying in some triangle $T \in \mathcal{T}$, such that z exists in η''' but not in η'' . In other words, we have $z = y_j y_{j+1} \cap y_k y_{k+1}$ for some j, k , whereas $x_j x_{j+1} \cap x_k x_{k+1} = \emptyset$. This means that one pair of vertices, say y_{j+1}, y_{k+1} , lie on the same edge $e_{j+1} = e_{k+1}$ of T and switched their order in the transition from η'' to η''' , while the other two vertices y_j, y_k lie on the two other edges of T , or else they both lie on the same edge of T but did not switch their order. Let $\ell \geq 1$ be the unique integer such that for all $1 \leq \ell' \leq \ell$, the vertices $y_{j+\ell'}, y_{k+\ell'}$ lie on the same edge $e_{j+\ell'} = e_{k+\ell'}$ and switched order, while this is not true of $y_{j+\ell+1}, y_{k+\ell+1}$. Note that no pair of vertices $(y_{j+\ell'}, y_{k+\ell'})$, $1 \leq \ell' \leq \ell$ can be ε -close to each other, because then we would not have switched their order when transforming η'' into η''' .

For each index m' , let $s_{m'}, t_{m'}$ be the segments $s_{m'} = x_{m'} x_{m'+1}$ and $t_{m'} = y_{m'} y_{m'+1}$. Then for all $1 \leq \ell' < \ell$, either none or both of the self-intersections $s_{j+\ell'} \cap s_{k+\ell'}, t_{j+\ell'} \cap t_{k+\ell'}$ exist. In contrast, exactly one of the self-intersections $s_{j+\ell} \cap s_{k+\ell}, t_{j+\ell} \cap t_{k+\ell}$ exists. Meaning, we have associated the self-intersection z that was *created* to another self-intersection z' that was either *created* or *destroyed*. See Figure 12 (top). Furthermore, this association is one-to-one, since, if z' was also created, then it is associated back to z . We now show that z' must have been destroyed, not created.

Suppose for a contradiction that the self-intersection z' was also created. We will use a mix-and-match argument in order to arrive at a contradiction to the fact that η''' is within ε of being homotopically shortest. The mix-and-match consists of interchanging the positions of $y_{j+\ell'}$ and $y_{k+\ell'}$ for all $1 \leq \ell' \leq \ell$ (see Figure 12, bottom). But in order for the mix-and-match argument to be valid, we need to show that the portion of η''' between y_j and $y_{j+\ell}$ is parametrically disjoint from the portion between y_k and $y_{k+\ell}$, or in other words, the indices $j, j + \ell, k, k + \ell$ lie in this circular order. We leave this detail to the end.

Let L_1, L_2 be the length of the portions of η''' between y_j and $y_{j+\ell+1}$, and between y_k and $y_{k+\ell+1}$, respectively. Suppose first that for at least one of the pairs $(y_j, y_k), (y_{j+\ell+1}, y_{k+\ell+1})$, the two points are separated by distance larger than ε . In this case, if we interchange the positions of $y_{j+\ell'}$ and $y_{k+\ell'}$ (which, as mentioned before, are separated by distance larger than ε) for all $1 \leq \ell' \leq \ell$, then $L_1 + L_2$ decreases significantly (by an amount that does not tend to 0 with ε). This contradicts the assumption that η''' is ε -close to the shortest homotopic curve γ' .

Now suppose (y_j, y_k) are ε -close to each other, as well as $(y_{j+\ell+1}, y_{k+\ell+1})$. If L_1 is significantly different from L_2 (by an amount that does not tend to 0 with ε), say with $L_1 > L_2$, then we could have moved each $y_{j+\ell'}$ to within ε of $y_{k+\ell'}$, lowering L_1 to L_2 and making η''' shorter. And if L_1 is almost equal to L_2 then, letting $\varepsilon \rightarrow 0$ we obtain a counterexample to the uniqueness of the

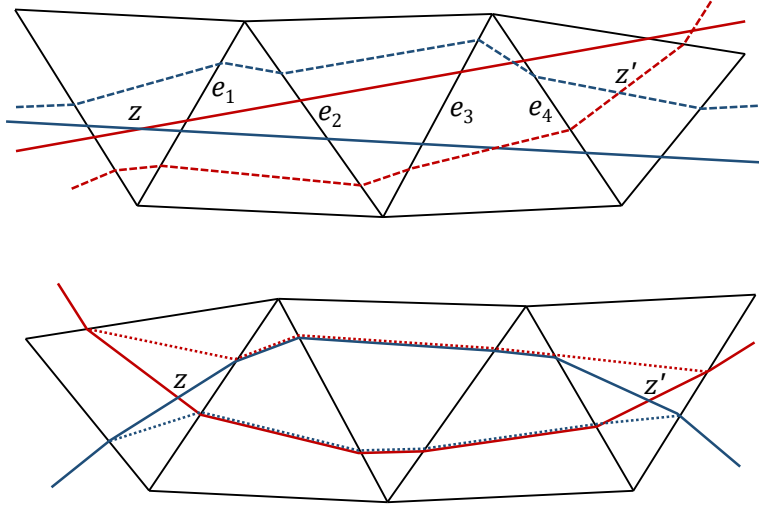


Figure 12: Top: In the transition from η'' (dashed curves) to η''' (solid curves), vertices at e_1, e_2, e_3, e_4 had their order swapped, so self-intersection z was created while self-intersection z' was destroyed. Bottom: If both z and z' were created, then interchanging the position of the intermediate vertices eliminates both self-intersections, and also produces a shorter curve.

shortest homotopic path from y_j to $y_{j+\ell+1}$. This finishes our mix-and-match argument.

Now we prove that the indices $j, j + \ell, k, k + \ell$ lie in this circular order, as promised. Suppose for a contradiction that $j < k \leq j + \ell$. Then the edges e_{j+1}, \dots, e_k are the same as the edges e_{k+1}, \dots, e_{2k-j} , meaning, the curve η''' winds twice in a row along the same edges. But then, by a result of Hershberger and Snoeyink [28], which we call the *two windings lemma* and include in Appendix B, y_{j+u} must be ε -close to y_{k+u} for some $1 \leq u \leq k - j$. This is a contradiction, as mentioned above.

This concludes the proof of Theorem 6 for the case of the number of self-intersections of a single curve. The case of the number of intersections of two curves is similar, though slightly simpler since there is no need to invoke the two windings lemma. \square

Theorem 7. *For a fixed obstacle set P , the P -curve that maximizes the number of HCS iterations is the boundary of the convex hull of P .*

Proof. Let γ_0 be a given P -curve, and let δ_0 be the boundary of the convex hull of P . The curves γ_0 and δ_0 are disjoint, and furthermore, their separation into disjoint $\widehat{\gamma}_0, \widehat{\delta}_0$ can be done in such a way that $\widehat{\gamma}_0$ lies on the bounded side of $\widehat{\delta}_0$. We say for short that δ_0 bounds γ_0 . Let $\gamma_{i+1} = \text{HCS}_P(\gamma_i)$ and $\delta_{i+1} = \text{HCS}_P(\delta_i)$ for all i . The proof of Theorem 6 describes how to obtain disjoint $\widehat{\gamma}_{i+1}, \widehat{\delta}_{i+1}$ that are ε -close to $\gamma_{i+1}, \delta_{i+1}$, from the corresponding curves $\widehat{\gamma}_i, \widehat{\delta}_i$. Furthermore, each of the steps described in the proof (namely the snapping, edge-sequence reduction, and vertex sliding steps) conserves the property that $\widehat{\gamma}_i$ remains on the bounded side of $\widehat{\delta}_i$. Hence, δ_i bounds γ_i for all i . Therefore, the HCS process starting with γ_0 does not take more iterations than the one starting with δ_0 . \square

Theorem 8. *Let P be an obstacle set in general position. Let γ be a simple P -curve. Then $\text{HCS}_P(\gamma)$ is also simple. Let γ_1, γ_2 be disjoint P -curves. Then $\text{HCS}_P(\gamma_1), \text{HCS}_P(\gamma_2)$ are also disjoint. Hence, under HCS with obstacles in general position, a simple curve stays simple, and a pair of disjoint curves stay disjoint.*

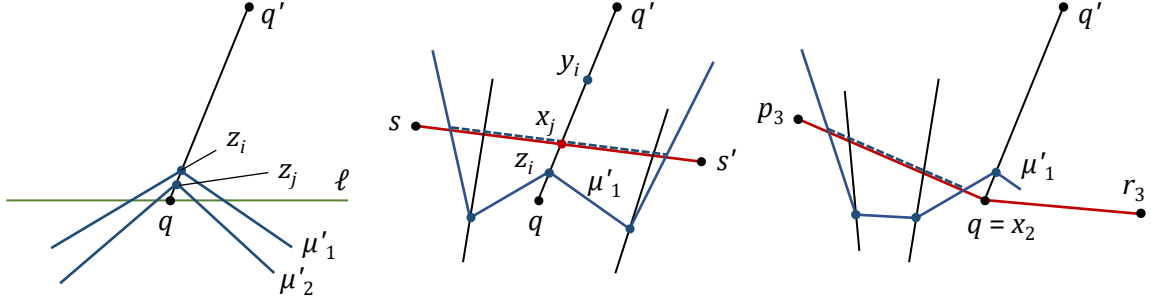


Figure 13: Left: Assuming for a contradiction that γ' visits an obstacle q twice. Center: The red segment ss' is part of γ , and η''' (blue) could be made shorter by taking the dashed shortcut. Right: The red segments p_3qr_3 are part of γ , and again η''' (blue) could be made shorter by taking the dashed shortcut.

Proof. Let P be in general position, let \mathcal{T} be a triangulation of P , and let γ be a simple P -curve. Suppose that $\gamma' = \text{HCS}_P(\gamma)$ did not collapse to a point. We will show that γ' is also simple. Let $\eta, \eta', \eta'', \eta'''$ be as in the proof of Theorem 6; see again Table 2.

Let (e_0, \dots, e_{m-1}) be the circular list of edges visited by η'' and η''' . For each $0 \leq i < m$, let y_i be the vertex of η'' on e_i , and let z_i be the vertex of η''' on e_i . Hence, η'' was transformed into η''' by sliding each y_i to z_i along e_i .

We already know that η''' is simple, and so no two vertices y_i on the same edge switched order during the sliding. Hence, all we need to show is that γ' does not visit any vertex twice.

Suppose for a contradiction that $q \in P$ is visited twice by γ' , with the two visits being $\mu_1 = p_1qr_1$ and $\mu_2 = p_2qr_2$. Let μ'_1, μ'_2 be the portions of η''' corresponding to μ_1, μ_2 . Since η''' is simple and ε -close to shortest, there must exist a line ℓ through q such that p_1, r_1, p_2, r_2 all lie on one side of ℓ , and such that μ'_1, μ'_2 briefly cross to the other side of ℓ when going around p , before crossing back. See Figure 13 (left). Assume for simplicity that ℓ is horizontal, with p_1, r_1, p_2, r_2 below ℓ . Let $e = qq'$ be a triangulation edge with q' above ℓ . Let z_i, z_j be the vertices of η''' in $\mu'_1 \cap e, \mu'_2 \cap e$, respectively, where $e_i = e_j = e$. Assume without loss of generality that z_i lies higher than z_j .

The corresponding vertices y_i, y_j of η'' are ε -close to two points $x_i, x_j \in \gamma \cap e$, where x_i lies higher than x_j . The point x_j could be either the lower endpoint q or somewhere in the middle of e (it cannot be the upper endpoint q' since then we would also need to have $x_i = q$, so γ would self-intersect).

Suppose first that x_j is somewhere in the middle of e , so $x_j \in ss'$ for some $s, s' \in P$. The segment ss' cannot equal e , since then γ would self-intersect as before. Hence, y_i crossed ss' on its way to z_i . Let $i' \leq i$ and $i'' \geq i$ be minimal and maximal indices such that all the edges $e_{i'}, \dots, e_{i''}$ intersect ss' and the corresponding vertices $y_{i'}, \dots, y_{i''}$ crossed ss' on their way to $z_{i'}, \dots, z_{i''}$, in the transition from η'' to η''' . (The edges $e_{i'}, \dots, e_{i''}$ cannot be *all* the edges e_0, \dots, e_{m-1} , since then η'' would be collapsible to a point.) But then η''' could be made significantly shorter (by an amount that does not tend to 0 as $\varepsilon \rightarrow 0$) by not having these vertices cross ss' . See Figure 13 (center). Contradiction.

Now suppose $x_j = q$, so x_j is part of a visit p_3qr_3 of γ . The edge e must be on the side of at which the angle p_3qr_3 is less than 180 degrees. Hence, one of the points p_3, r_3 must be above ℓ . Say it is p_3 . Hence, the portion μ'_1 of η''' intersects p_3q , so so one or more consecutive vertices of η'' moved across p_3q in the transition from η'' to η''' . Thus, η''' could be made shorter by not crossing p_3q , as before. Contradiction.

The case of two curves is similar. □

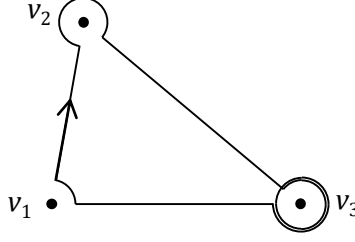


Figure 14: Type-1 curve with $\alpha_1 = 80^\circ$, $\alpha_2 = -300^\circ$, $\alpha_3 = -680^\circ$.

5.5 Proof of Theorem 9

In this section we prove Theorem 9, regarding the number of inflection edges. The proof is based on the vertex-release algorithm. The basic idea is that, given a self-disjoinable curve, if the vertex releases are performed in an appropriate order, then the curve stays self-disjoinable at all times. Moreover, no vertex release increases the number of inflection edges. Along the way, we develop enough machinery to re-prove Theorem 6.

We will use the type-2 curves introduced above. We also introduce two other types of curves that are arbitrarily close to P -curves. We call them *type-1* and *type-3* curves.

Type-1 curves. Let P be a set of obstacle points, let γ be a P -curve that goes through obstacles (p_0, \dots, p_{k-1}) in this circular order, and let $\varepsilon > 0$ be small enough. For each $p \in P$, let C_p be a circle of radius ε centered at p . A *type-1* curve δ corresponding to γ is composed of *straight parts* and *circular parts*. For each i , let e_i be the segment $p_{i-1}p_i$. Each straight part goes from the point $y_{i-1} = e_i \cap C_{p_{i-1}}$ to the point $x_i = e_i \cap C_{p_i}$. And each circular part goes along C_{p_i} from x_i to the next point y_i , either clockwise or counterclockwise, describing any number of turns around C_i .³ Hence, δ can be combinatorially specified by associating to each p_i a signed angle α_i that is congruent modulo 2π to $\angle p_{i-1}p_i p_{i+1}$. See Figure 14. The unique P -curve corresponding to a given type-1 curve δ is denoted by $t_P(\delta)$.

Type-3 curves. A *type-3* curve is an (ε^2) -perturbation of a type-1 curve. A type-3 curve is a self-transversal curve composed of *straight parts* and *spiral parts*. Each spiral part is centered at some $p \in P$, and its initial and final radii satisfy $\varepsilon < r_0 < r_1 < \varepsilon + \varepsilon^2$. The interval $[r_0, r_1]$ is called the *radial interval* of the spiral part. Different spiral parts centered at the same obstacle p have disjoint radial intervals. Furthermore, the endpoints of the spiral parts are displaced either clockwise or counterclockwise by distance up to ε^2 from the corresponding endpoints in the type-1 curve. It does not matter whether the spiral parts spiral out clockwise or counterclockwise, since the number of self-intersections is unaffected.

Hence, a type-3 curve can be specified purely combinatorially, by specifying, for each obstacle $p \in P$, the relative order of the radial intervals of the spiral parts around p , and for each other obstacle $q \neq p$, the clockwise order of the endpoints near p of the straight parts that go between p and q . See Figure 15 for an example.

More generally, we define a *collection of type-3 curves* on the same obstacle set, and we specify their relation to one another purely combinatorially in a similar way.

Each type-3 curve ζ corresponds (is (ε^2) -close) to a unique type-1 curve, which we denote by $t_1(\zeta)$. We also define $t_P(\zeta)$ as $t_P(t_1(\zeta))$.

³The circular parts can be approximated arbitrarily closely by piecewise-linear paths.

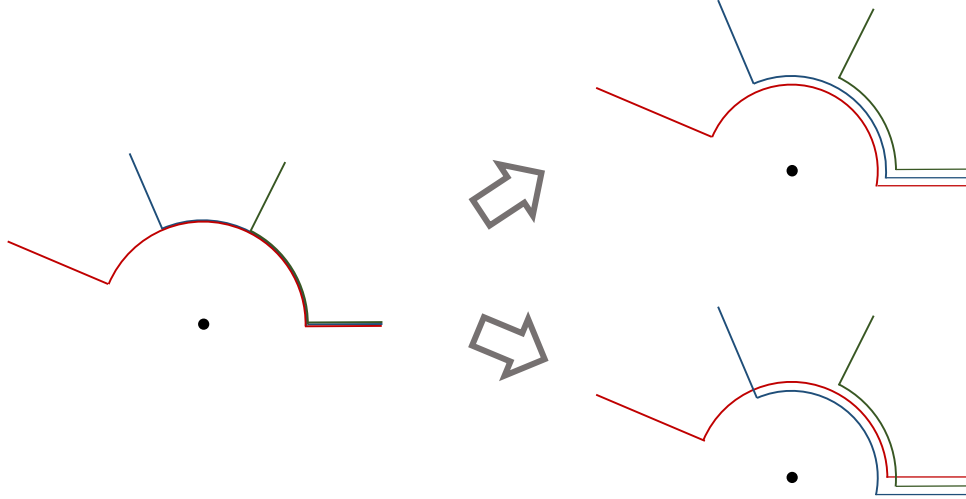


Figure 15: Two different type-3 realizations of the same type-1 curve. The type-1 curve in this example visits the shown obstacle three times. The three visits are shown in different colors.

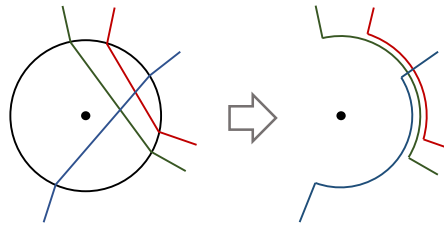


Figure 16: Turning a type-2 curve into a type-3 curve.

Observation 12. *Let δ be a self-transversal type-2 curve. Then δ can be turned into a self-transversal type-3 curve ζ ε -close to it, such that their number of self-intersections satisfy $\chi(\zeta) = \chi(\delta)$. Similarly, let δ_1, δ_2 be transversal type-2 curves. Then they can be turned into transversal type-3 curves ζ_1, ζ_2 ε -close to them whose number of intersections satisfy $\chi(\zeta_1, \zeta_2) = \chi(\delta_1, \delta_2)$.*

Proof. Assume without loss of generality that the given type-2 curves do not pass through any $p \in P$. We turn the short parts of the type-2 curves into spiral parts of type-3 curves. The shorter the part, the larger the radius. See Figure 16. The number of intersections stays unchanged. \square

Let γ be a P -curve, let δ be a type-2 curve corresponding to γ , and let ζ be the type-3 curve obtained from δ as in Observation 12. For every nailed visit that γ makes to an obstacle $p \in P$, the corresponding type-3 curve ζ has a corresponding visit to p with a spiral part that describes an angle very close to π . We call this visit of ζ *nailed*. Call a type-3 curve *steady* if, for every $p \in P$, the nailed spiral parts around P have smaller radii than the non-nailed ones. Then our curve ζ is steady by construction.

A visit of a type-3 curve to an obstacle $p \in P$ is called *stable* (resp. *unstable*) if the visit of the corresponding type-1 curve to p is stable (resp. unstable).

In order to release an unstable visit to an obstacle p in a type-3 curve, we proceed as in the type-1 curve it realizes, and then we decide on the radius and endpoint order of the spiral parts that were newly created or modified. If p is both preceded and followed by the same obstacle q ,

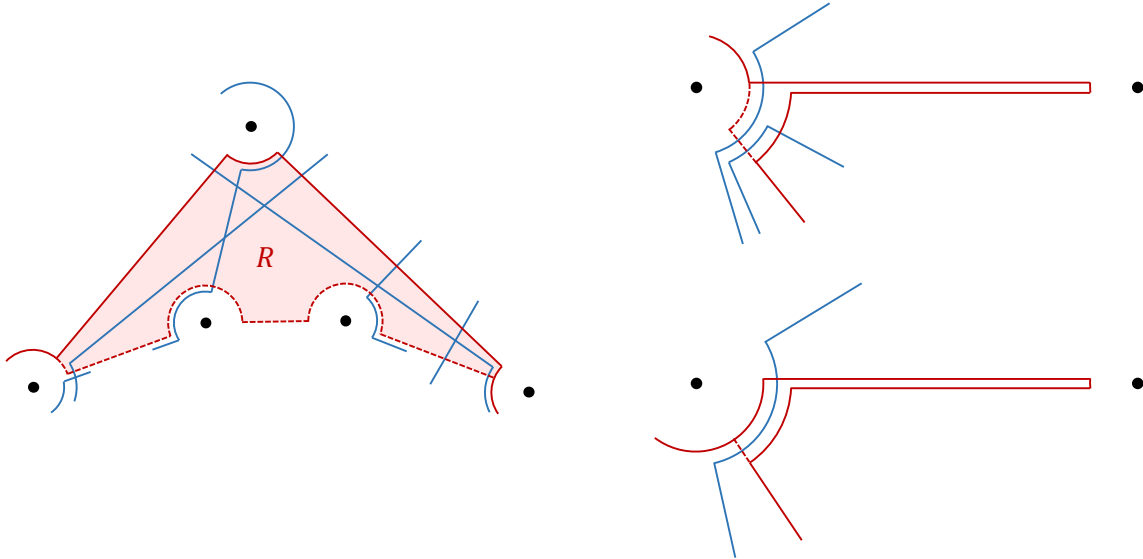


Figure 17: Vertex releases on type-3 curves. In each example, the red curve undergoes a vertex release. The dotted curves are the resulting curves after the release. The blue curves are examples of other curves (of portions thereof) present in the vicinity. As a case analysis shows, whenever a blue curve intersects the red curve after the release, the two curves also intersected before the release.

recall that we merge the two visits of q . If at least one of these visits was nailed, then we mark the new visit as nailed.

Lemma 13. *Let γ be a steady type-3 curve with at least one unstable, non-nailed obstacle visit. Then there is a way to perform a vertex release on one such visit, such that the number of self-intersections does not increase, and such that the resulting curve is also steady.*

Proof. Let p be an obstacle that has at least one unstable non-nailed visit. Release, from among all unstable visits to p , the one v_i with the largest radius in γ . Suppose first that v_{i-1} and v_{i+1} visit different obstacles. In each new obstacle visit w_k , we give the new spiral part the largest radius around in that obstacle. The relative order of the starting and ending points of that spiral part are chosen so that the spiral part is as short as possible. The spiral part of v_{i-1} has an endpoint a that stays in place and an endpoint b that moves. The new position of the endpoint b is chosen as close as possible to its old position. The same is done for v_{i+1} .

Hence, a piece γ_{old} of γ is replaced by another piece γ_{new} , and $\gamma_{\text{old}}, \gamma_{\text{new}}$ together form a simple curve, bounding a region R . See Figure 17 (left). The number of self-intersections does not increase, since any other curve piece that enters R by crossing γ_{new} , must exit R by crossing γ_{old} .

If v_{i-1} and v_{i+1} visit the same obstacle q , then there are two spiral parts c_1, c_2 around q that are merged into one. We give the new spiral part the smaller radius among the old radii of c_1, c_2 . This way, the resulting curve is also steady. Further, a case analysis shows that the number of self-intersections does not increase. See Figure 17 (right). \square

Lemma 13 provides an alternative proof of Theorem 6: We repeatedly release non-nailed unstable vertices according to the lemma, until no such vertices remain.

Lemma 14. *Let C be a circle, let p, r be points on C , and let q be a point in the interior of the disk bounded by C . Suppose the ordered triple p, q, r describes a clockwise (resp. counterclockwise)*

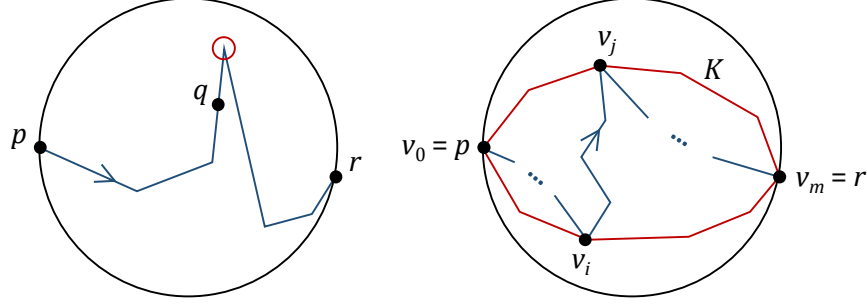


Figure 18: Left: A simple path from p through q to r that does not leave the circle must contain at least one clockwise vertex (marked in red). Right: Proof of the claim: The path must turn clockwise at v_j .

turn. Let γ be a simple piecewise-linear path that goes from p through q to r and does not otherwise intersect C . Then γ has at least one clockwise (resp. counterclockwise) vertex. See Figure 18 (left).

Proof. Let K be the boundary of the convex hull of γ . Let v_0, \dots, v_{n-1} be the vertices of K in counterclockwise order, with $v_0 = p$. Let m be such that $v_m = r$. Let v_j be the first vertex with $m < j < n$ visited by γ , and let v_i be the last vertex with $0 \leq i < m$ visited by γ before v_j . Then the subpath of γ from v_i to v_j , together with the part of K counterclockwise from v_i to v_j , form a simple closed curve, which γ cannot cross. Since γ must end at $r = v_m$, it must turn clockwise at v_j . See Figure 18 (right). \square

Let γ be a self-disjoinable P -curve, and let δ be a simple type-3 curve realizing γ . (We know such a δ exists by Lemma 11 and Observation 12.) Let (p_0, \dots, p_k) be the minimal sequence of vertices of γ (i.e. this sequence omits obstacles at which γ continues in a straight line). For each i , let e_i be the edge $e_i = p_{i-1}p_i$. We will define the notion of an edge e_i being realized by δ as an inflection edge. For this, we first define the notion of a vertex p_i being realized by δ as a clockwise (counterclockwise) turn. If p_{i+1} lies to the right (resp. left) of the directed edge e_i , then we say that p_i is realized by δ as a clockwise (resp. counterclockwise) turn, irrespective of δ . Now suppose p_{i+1} lies on the ray emanating from p_i through p_{i-1} (so γ makes a U-turn at p_i). Let q_i be the obstacle point visited by γ right before and after p_i (note that q_i is not necessarily a vertex of γ). Let L_i, L'_i be the long parts of δ corresponding to the segments $q_i p_i, p_i q_i$ of γ , respectively. If L'_i lies to the right of L_i (considering L_i as a directed segment), then we say that p_i is realized by δ as a clockwise turn. Otherwise, we say that p_i is realized by δ as a counterclockwise turn. The turning direction of the spiral parts of δ are irrelevant for this definition. Finally, we say that an edge e_i is realized by δ as an inflection edge if one of p_{i-1}, p_i is realized by δ as a clockwise turn and the other one as a counterclockwise turn. Denote by $\iota_\gamma(\delta)$ the number of edges of γ that are realized by δ as inflection edges.

For every obstacle q at which γ continues in a straight line, we say that δ is *straight* at q .

Theorem 9. *Let γ be self-disjoinable, and let $\gamma' = \text{HCS}_P(\gamma)$. Then their inflection-edge numbers satisfy $\iota(\gamma') \leq \iota(\gamma)$. Hence, under HCS on a self-disjoinable curve, the curve's number of inflection edges never increases.*

Proof. Let γ be a self-disjoinable P -curve, and let $\gamma' = \text{HCS}_P(\gamma)$. Let $\varepsilon > 0$ be small enough. Let $\hat{\gamma}$ be a simple piecewise-linear curve (ε^2)-close to γ minimizing the number of inflection edges $\iota(\hat{\gamma})$. We will construct a simple piecewise-linear curve ρ that is ε -close to γ' and satisfies $\iota(\hat{\gamma}) \geq \iota(\rho)$.

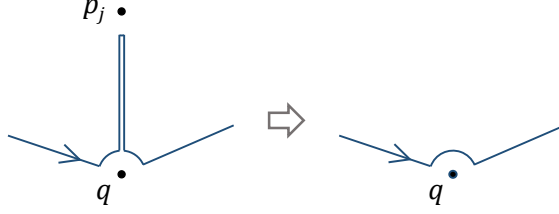


Figure 19: When releasing a vertex p_j that makes a clockwise U-turn, if after the release the curve makes a counterclockwise turn at q , then before the release both visits to q were counterclockwise.

Let $\delta = \text{snap}(\widehat{\gamma})$. By Lemma 11, δ is also simple. Let ζ be the type-3 curve obtained from δ according to the procedure in Observation 12. Then ζ is simple as well. Consider a vertex p_i of γ that is realized by ζ as a clockwise turn. By the construction of δ and ζ and by Lemma 14, $\widehat{\gamma}$ must have a clockwise vertex inside the circle C_{p_i} . Similarly, if p_i is realized by ζ as a counterclockwise turn, then $\widehat{\gamma}$ must have a counterclockwise vertex inside C_{p_i} . Hence, $\iota(\widehat{\gamma}) \geq \iota_\gamma(\zeta)$.

Now repeatedly release non-nailed unstable obstacle visits from ζ as in Lemma 13, until none remain, obtaining ζ' . Let ζ_0, \dots, ζ_k be the sequence of type-3 curves produced in this process, with $\zeta_0 = \zeta$ and $\zeta_k = \zeta'$. Then ζ_i is simple for each i . For each i , let $\gamma_i = t_P(\zeta_i)$. In particular, $\gamma' = \gamma_k$.

We claim that no vertex release increases the number of inflection edges, meaning $\iota_{\gamma_i}(\zeta_i) \geq \iota_{\gamma_{i+1}}(\zeta_{i+1})$ for all i .

Indeed, consider the release of vertex p_j of γ_i . Say it is realized by ζ_i as a clockwise turn. Suppose first that γ_i does not make a U-turn at p_j . Then p_j is replaced in γ_{i+1} by zero or more new vertices, all of which are realized by ζ_{i+1} as clockwise turns. Let q, q' be the obstacles crossed by γ_i just before and after p_j , respectively. Then each of q, q' could change from counterclockwise to straight, or from counterclockwise to clockwise, or from straight to clockwise, or they could stay as they are. This is true even if one of γ_i, γ_{i+1} makes a U-turn at one or both of these vertices. Hence, the number of alternations between clockwise and counterclockwise did not increase at step i .

Now suppose that γ_i makes a U-turn at p_j . Let q be the obstacle that precedes and follows p_j in γ . Recall that in this case, the visit to p_j is removed and the two visits to q are merged into one. As before, here there are several options as to whether the visit(s) of q by γ_i, γ_{i+1} are straight, or are realized as counterclockwise or clockwise by ζ_i, ζ_{i+1} . However, if the visit of q by γ_{i+1} is realized as counterclockwise, then both visits by γ_i had to be realized as counterclockwise. See Figure 19. Hence, in this case as well, the number of alternations between clockwise and counterclockwise did not increase at step i . This finishes the proof that $\iota_{\gamma_i}(\zeta_i) \geq \iota_{\gamma_{i+1}}(\zeta_{i+1})$ for each i . Hence, $\iota_\gamma(\zeta) \geq \iota_{\gamma'}(\zeta')$.

Next, we turn ζ' into a type-2 curve ζ'' by reversing the procedure of Observation 12; namely, we turn the spiral parts of ζ' into straight segments, and we move the endpoints of these segments to distance ε of the corresponding obstacles. This does not introduce any self-intersections, so ζ'' is simple. There is a slight final problem: For each obstacle at which γ' goes straight, the corresponding short part of ζ'' might be an inflection edge. This problem is solved by straightening the appropriate portions of ζ'' as in Figure 20. Let ρ be the straightened curve. Then ρ is still simple, and no short part of ρ is an inflection edge. Hence, $\iota_{\gamma'}(\zeta') \geq \iota(\rho)$. Summing up, we have

$$\iota(\widehat{\gamma}) \geq \iota_\gamma(\zeta) \geq \iota_{\gamma'}(\zeta') \geq \iota(\rho),$$

concluding the proof. □

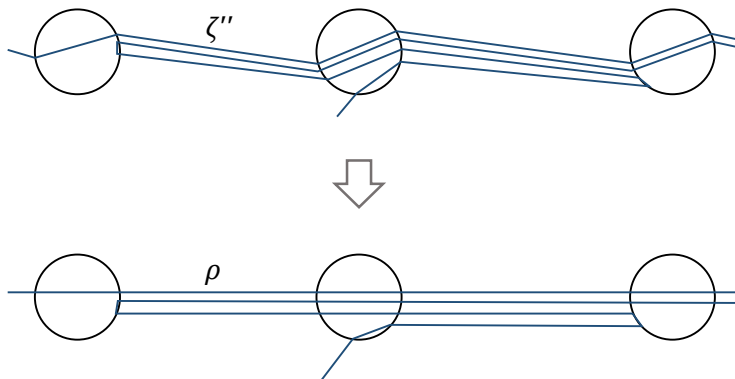


Figure 20: Removing slight inflection edges.

6 Discussion

One of the reasons continuous curve-shortening flows were introduced and studied was to overcome the shortcomings of the *Birkhoff curve-shortening process* ([9], see also e.g. [17]), specifically the fact that it might cause the number of curve intersections to increase [25, 27]. As we have shown, HCS is a discrete process that overcomes this flaw without introducing analytical difficulties, at least in the plane. We conjecture that the definition of HCS can be extended without modifications to more general surfaces. It would be interesting to check whether such an extension has the properties which HCS has in the plane. The answer might depend on the properties of the surface.

Acknowledgements. Thanks to Arseniy Akopyan, Imre Bárány, Jeff Erickson, Radoslav Fulek, Jeremy Schiff, Arkadiy Skopenkov, and Peter Synak for useful discussions. Thanks also to the referees for their useful comments.

References

- [1] Hugo A. Akitaya, Greg Aloupis, Jeff Erickson, and Csaba D. Tóth. Recognizing weakly simple polygons. *Discrete & Computational Geometry*, 58:785–821, 2017.
- [2] Hugo A. Akitaya, Radoslav Fulek, and Csaba D. Tóth. Recognizing weak embeddings of graphs. In *Proc. 29th Symp. on Discrete Algorithms*, pages 274–292, 2018. doi:10.1137/1.9781611975031.20.
- [3] Steven J. Altschuler and Matthew A. Grayson. Shortening space curves and flow through singularities. *J. Differential Geom.*, 35(2):283–298, 1992. doi:10.4310/jdg/1214448076.
- [4] Luis Alvarez, Frédéric Guichard, Pierre-Luis Lions, and Jean-Michel Morel. Axioms and fundamental equations of image processing. *Arch. Rational Mech. Anal.*, 123(3):199–257, 1993. doi:10.1007/BF00375127.
- [5] Sigurd Angenent. Parabolic equations for curves on surfaces: Part II. Intersections, blow-up and generalized solutions. *Annals of Mathematics*, 133(1):171–215, 1991. doi:10.2307/2944327.

- [6] Sigurd Angenent, Guillermo Sapiro, and Allen Tannenbaum. On the affine heat equation for non-convex curves. *J. Amer. Math. Soc.*, 11(3):601–634, 1998. doi:10.1090/S0894-0347-98-00262-8.
- [7] Vic Barnett. The ordering of multivariate data. *J. Roy. Statist. Soc. Ser. A*, 139(3):318–355, 1976. doi:10.2307/2344839.
- [8] Sergei Bespamyatnikh. Computing homotopic shortest paths in the plane. *Journal of Algorithms*, 49(2):284–303, 2003. doi:https://doi.org/10.1016/S0196-6774(03)00090-7.
- [9] George D. Birkhoff. Dynamical systems with two degrees of freedom. *Trans. Amer. Math. Soc.*, 18:199–300, 1917.
- [10] Sergio Cabello, Yuanxin Liu, Andrea Mantler, and Jack Snoeyink. Testing homotopy for paths in the plane. *Discrete & Computational Geometry*, 31(1):61–81, 2004. doi:10.1007/s00454-003-2949-y.
- [11] Jeff Calder and Charles K. Smart. The limit shape of convex hull peeling. *Duke Math. J.*, 169(11):2079–2124, 2020. doi:10.1215/00127094-2020-0013.
- [12] Frédéric Cao. *Geometric Curve Evolution and Image Processing*, volume 1805 of *Lecture Notes in Mathematics*. Springer-Verlag, Berlin, 2003. doi:10.1007/b10404.
- [13] Hsien-Chih Chang and Jeff Erickson. Untangling planar curves. *Discrete & Computational Geometry*, 58:889–920, 2017. doi:10.1007/s00454-017-9907-6.
- [14] Bernard Chazelle. A theorem on polygon cutting with applications. In *Proc. 23rd Annual Symposium on Foundations of Computer Science (FOCS 1982)*, pages 339–349, 1982. doi:10.1109/SFCS.1982.58.
- [15] Bernard Chazelle. On the convex layers of a planar set. *IEEE Trans. Inform. Theory*, 31(4):509–517, 1985. doi:10.1109/TIT.1985.1057060.
- [16] Kai-Seng Chou and Xi-Ping Zhu. *The Curve Shortening Problem*. Chapman & Hall/CRC, Boca Raton, FL, 2001. doi:10.1201/9781420035704.
- [17] Cristopher B. Croke. Area and the length of the shortest closed geodesic. *J. Differential Geometry*, 27:1–21, 1988.
- [18] Ketan Dalal. Counting the onion. *Random Struct. Algor.*, 24(2):155–165, 2004. doi:10.1002/rsa.10114.
- [19] William F. Eddy. Convex Hull Peeling. In *COMPSTAT 1982 5th Symposium held at Toulouse 1982*, pages 42–47. Physica-Verlag, 1982. doi:10.1007/978-3-642-51461-6_4.
- [20] Alon Efrat, Stephen G. Kobourov, and Anna Lubiw. Computing homotopic shortest paths efficiently. *Computational Geometry*, 35(3):162–172, 2006. doi:https://doi.org/10.1016/j.comgeo.2006.03.003.
- [21] David Eppstein, Sariel Har-Peled, and Gabriel Nivasch. Grid peeling and the affine curve-shortening flow. *Experimental Mathematics*, page to appear, 2018. https://doi.org/10.1080/10586458.2018.1466379. doi:10.1080/10586458.2018.1466379.

- [22] Radoslav Fulek and Csaba D. Tóth. Crossing minimization in perturbed drawings. In T. Biedl and A. Kerren, editors, *Proc. 26th Symp. Graph Drawing and Network Visualization*, pages 229–241. Springer, 2018. doi:10.1007/978-3-030-04414-5_16.
- [23] Michael Gage and Richard S. Hamilton. The heat equation shrinking convex plane curves. *J. Differential Geom.*, 23(1):69–96, 1986. doi:10.4310/jdg/1214439902.
- [24] Matthew A. Grayson. The heat equation shrinks embedded plane curves to round points. *J. Differential Geom.*, 26(2):285–314, 1987. doi:10.4310/jdg/1214441371.
- [25] Matthew A. Grayson. Shortening embedded curves. *Annals of Mathematics*, 129(1):79–111, 1989.
- [26] Sarel Har-Peled and Bernard Lidický. Peeling the grid. *SIAM J. Discrete Math.*, 27(2):650–655, 2013. doi:10.1137/120892660.
- [27] Joel Hass and Peter Scott. Shortening curves on surfaces. *Topology*, 33:25–43, 1994. doi:10.1016/0040-9383(94)90033-7.
- [28] John Hershberger and Jack Snoeyink. Computing minimum length paths of a given homotopy class. *Computational Geometry*, 4(2):63–97, 1994. doi:https://doi.org/10.1016/0925-7721(94)90010-8.
- [29] Der-Tsai Lee and Franco P. Preparata. Euclidean shortest paths in the presence of rectilinear barriers. *Networks*, 14(3):393–410, 1984. doi:10.1002/net.3230140304.
- [30] Charles E. Leiserson and F. Miller Maley. Algorithms for routing and testing routability of planar VLSI layouts. In Robert Sedgwick, editor, *Proceedings of the 17th Annual ACM Symposium on Theory of Computing*, pages 69–78. ACM, 1985. doi:10.1145/22145.22153.
- [31] Guillermo Sapiro and Allen Tannenbaum. Affine invariant scale-space. *Int. J. Comput. Vision*, 11(1):25–44, 1993. doi:10.1007/bf01420591.
- [32] Brian White. Evolution of curves and surfaces by mean curvature. In *Proceedings of the International Congress of Mathematicians, Vol. I (Beijing, 2002)*, pages 525–538, 2002. URL: <https://www.mathunion.org/fileadmin/ICM/Proceedings/ICM2002.1/ICM2002.1.ocr.pdf>.
- [33] E. C. Zeeman. Relative simplicial approximation. *Mathematical Proceedings of the Cambridge Philosophical Society*, 60(1):39–43, 1964. doi:10.1017/S0305004100037415.

A Uniqueness of shortest homotopic curve

The following lemma is included for completeness.

Lemma 15. *Let P be a set of polygonal and point obstacles, and let γ be a path or curve that avoids P (except possibly at the endpoints). Then there exists a unique path or curve δ homotopic to γ that is locally shortest.*

Proof. The basic idea is that length function on the space of piecewise-linear curves is convex.

We use the triangulation approach of Section 5.1. Suppose for a contradiction that δ_1 and δ_2 are two different locally shortest curves or paths homotopic to γ . Clearly, their edge sequences must

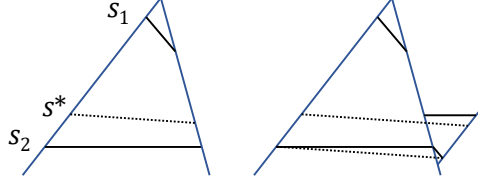


Figure 21: Proof of an inequality involving the lengths of three segments.

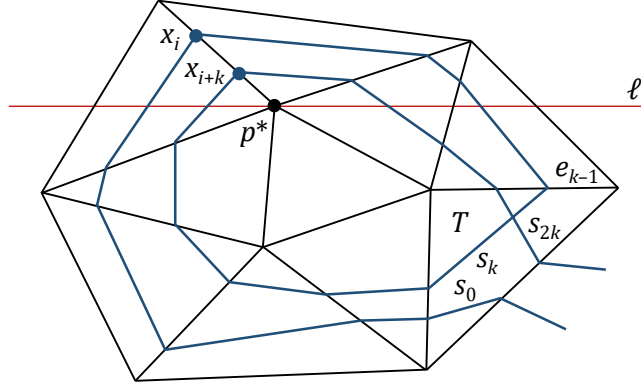


Figure 22: Proof of the two windings lemma.

be reduced, so we have $\mathcal{E}(\delta_1) = \mathcal{E}(\delta_2)$. Denote this common edge sequence by \mathcal{E} . All vertices of δ_1, δ_2 must lie on edges of \mathcal{E} . For each $e \in \mathcal{E}$, let $x_{e,1}, x_{e,2}$ be the vertex of δ_1, δ_2 on e , respectively. Say the lengths of the curves satisfy $|\delta_1| \geq |\delta_2|$.

Given $\varepsilon > 0$, for each $e \in \mathcal{E}$ define the point $x_e^* = (1 - \varepsilon)x_{e,1} + \varepsilon x_{e,2}$. Let δ^* be the curve or path that uses the sequence of points x_e^* as vertices. Clearly, δ^* is homotopic to γ . For each two adjacent edges $e_1, e_2 \in \mathcal{E}$, the corresponding curve segments s_1, s_2, s^* satisfy $|s^*| + (\varepsilon/(1 - \varepsilon))|s_2| \leq |s_1| + (\varepsilon/(1 - \varepsilon))|s_2|$ (see Figure 21), which implies $|s^*| \leq (1 - \varepsilon)|s_1| + \varepsilon|s_2|$. Hence, $|\delta^*| \leq (1 - \varepsilon)|\delta_1| + \varepsilon|\delta_2| \leq |\delta_1|$. This is true for all $\varepsilon > 0$, contradicting the assumption that δ_1 is locally shortest. \square

B The two windings lemma

The following fact that was stated and proven in [28] in a somewhat different context. We include the proof for completeness.

Lemma 16. *Let P be a finite set of obstacle points. Let \mathcal{T} be a triangulation of P . Let γ be a piecewise-linear curve that avoids P , such that its edge sequence $\mathcal{E}(\gamma) = (e_0, \dots, e_{m-1})$ is reduced (meaning, $e_i \neq e_{i+1}$ for all i). Suppose that there exists $k \leq m/2$ such that $e_i = e_{i+k}$ for all $0 \leq i < k$. (Meaning, γ winds twice in a row along a certain sequence of edges, and then does some other stuff before returning to its starting point.)*

Let δ be the shortest curve homotopic to γ . Let (x_0, \dots, x_{m-1}) be the vertices of δ , with $x_i \in e_i$ for each $0 \leq i < m$. Then there exists some $0 \leq i < k$ for which $x_i = x_{i+k}$.

Proof. For each i , let s_i be the segment $s_i = x_{i-1}x_i$ of δ . Note that the three segments s_0, s_k, s_{2k} lie in the same triangle $T \in \mathcal{T}$. Suppose without loss of generality that the edge $e_{k-1} = e_{2k-1}$

is horizontal and T lies below it. For each i , let $p_i \in P$ be the lower endpoint of the edge e_i (breaking ties arbitrarily). Let p^* be the highest point among $\{p_0, \dots, p_{k-1}\}$. Let ℓ be a horizontal line through p^* . Then the part of γ between e_0 and e_{k-1} crosses ℓ upwards, then crosses at least one non-horizontal edge e_i that has $p_i = p^*$, and then crosses ℓ' downwards. Hence, γ can be shortened by not rising above ℓ' , and therefore, in δ we have $x_i = p_i = p^*$. The same argument yields $x_{i+k} = p_{i+k} = p^*$. See Figure 22. \square

C Implementation details

Following [21], we simulated ACSF on the curve Δ of Section 3.1 using a simple front-tracking approach: We initially sampled $m = 1000$ points uniformly spaced along Δ . For each such point p_i , we estimate its normal vector and radius of curvature by the normal vector v_i and radius r_i of the unique circle passing through points p_{i-1}, p_i, p_{i+1} . We simultaneously let all points move at the appropriate speeds for a short time interval $t = \min\{c \cdot (d_{\min})^{4/3}, t_{\min}\}$, where d_{\min} is the minimum distance between two consecutive points, and $c = 3 \cdot 10^{-4}$ and $t_{\min} = 3 \cdot 10^{-9}$ are fixed parameters. Hence, as the minimum distance between points decreases, we take smaller time steps, except that we fix a minimum time step t_{\min} in order to be able to go past the singularity at which the self-intersection disappears. In order to prevent the points p_i from bunching together at sharp bends of the curve, each point p_i is also given a tangential velocity that tends to move it away from its closer neighbor among p_{i-1}, p_{i+1} . These tangential velocities should not affect the evolution of the flow, since they only cause the curve points to move within the curve.

We simulated HCS on uniform-grid obstacles and on random obstacles using two different programs. Both programs use the vertex-release method described in Section 5.2. The random-obstacle program stores points in a quadtree, in order to be able to answer triangle-containment queries efficiently. The random-obstacle program does not handle nailed obstacles, since in theory they occur with probability zero.

The uniform-grid program is more memory-efficient than the random-obstacle program, since it does not need to store all obstacles in memory, but rather takes the obstacle set to be \mathbb{Z}^2 . Vertex releases on the curve γ are performed as follows: Let p, q, r be three consecutive obstacles along γ , where q is to be released, and assume these three points do not lie on the same line. Note that the vectors $q - p, r - q$ are primitive (i.e. each one has relatively prime coordinates). Let z_1, \dots, z_k be the points that should replace q after the vertex release. Denote $z_0 = p, z_{k+1} = r$. Then each of the triangles $z_i q z_{i+1}$ has area $1/2$. Hence, given z_i and q , we can find z_{i+1} by an application of the extended Euclidean gcd algorithm, plus some additional calculations. We leave the details to the reader.

Our code is available at the following links:

<https://github.com/savvakumov/ACSF-simulation>

<https://github.com/savvakumov/HCS-with-random-obstacles>

<https://github.com/savvakumov/HCS-square-grid>